

Learning under Storage and Privacy Constraints

Berivan Isik

Department of Electrical Engineering
Stanford University
berivan.isik@stanford.edu

Tsachy Weissman

Department of Electrical Engineering
Stanford University
tsachy@stanford.edu

Abstract—Storage-efficient privacy-guaranteed learning is crucial due to enormous amounts of sensitive user data required for increasingly many learning tasks. We propose a framework for reducing the storage cost while at the same time providing privacy guarantees, without essential loss in the utility of the data for learning. Our method comprises noise injection followed by lossy compression. We show that, when appropriately matching the lossy compression to the distribution of the added noise, the compressed examples converge, in distribution, to that of the noise-free training data. In this sense, the utility of the data for learning is essentially maintained, while reducing storage and privacy leakage by quantifiable amounts. We present experimental results on the CelebA dataset for gender classification and find that our suggested pipeline delivers in practice on the promise of the theory: the individuals in the images are unrecognizable (or less recognizable, depending on the noise level), overall storage of the data is substantially reduced, with no essential loss of the classification accuracy. As an added bonus, our experiments suggest that our method yields a substantial boost to robustness in the face of adversarial test data.

Index Terms—compression-based denoising, rate-distortion theory, empirical distribution, learning,

I. INTRODUCTION

One of the most crucial factors contributing to the recent success of machine learning is the wide availability of user data [1]. However, relying on such data brings several challenges in storage and user privacy. While privacy-preserving methods for machine learning have been studied extensively, efficient storage of data for learning (a major problem even for synthetic datasets such as ImageNet [2] and CelebA [3]) remains largely unexplored. In this work, we propose a framework to tackle the two problems jointly. We seek to develop a storage-efficient privacy-guaranteeing processing procedure that preserves the utility of the data for learning.

To achieve this goal, we first inject noise N to the (learning data) examples X and then lossily compress the noisy examples Z (see Fig. 1). The reconstructions from the lossy compression of noisy (LCoN) examples \hat{X} are then used for the learning. The lossy compression is done under a distortion criterion and level that are matched to the noise characteristics in a way we prescribe below. For data efficiency, we aim to achieve a compression rate close to the optimum, as characterized by the rate-distortion function associated with the noisy data. As for privacy, following [4, 5, 6, 7, 8, 9, 10] and references therein, we guarantee an upper bound on the privacy leakage as measured by mutual information between the original data X and that retained \hat{X} .

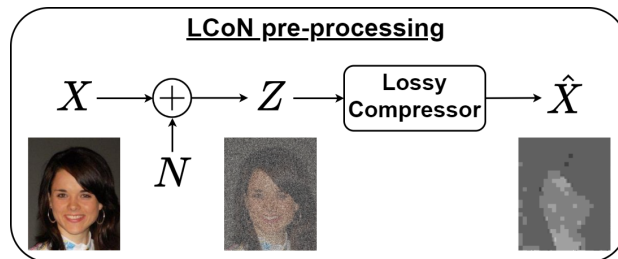


Fig. 1. Proposed data pre-processing framework. X : noise-free data, N : added noise, Z : noisy data, \hat{X} : reconstructions from lossy compression of the noisy data. \hat{X} are then used for the learning, in lieu of X . A sample of noise-free, noise-injected, and lossily compressed images from the CelebA dataset are given at the bottom. Here JPEG compression with quality factor 1 is applied to noisy images with 12 dB PSNR.

We show that this procedure achieves our goal, which might seem surprising at first glance in light of results from the literature on privacy and robustness showing significant degradation in performance of the trained model when data are corrupted by noise [11, 12]. Nevertheless, in a sense we make precise, this problem is alleviated in our framework due to the effective denoising that occurs when noisy data are lossily compressed. More concretely, when the distortion criterion and level in the lossy compression are matched to the noise characteristics, the lossily compressed noisy data samples converge, in distribution, to that of the noise-free data because, in effect, they are samples from the posterior distribution of the noise-free data given its noise-corrupted versions. The learning then is performed on data with the “right” statistics so, in principle, should entail no performance loss in the downstream inference tasks.

Our initial experimentation with gender classification on the CelebA dataset seems in agreement with the theory. For example, one working point of our method decreases the cost of storing the data (in bits) by a factor of two, provides privacy guarantees by adding Gaussian noise (with varying variance where the individuals in the noisy images were unrecognizable by the authors), while achieving better accuracy than the benchmark methods. Furthermore, our method yields substantial performance boosts over the benchmark methods when tested on adversarially generated data.

Our main contributions can be summarized as:

- 1) We propose a framework for data-efficient privacy-preserving pre-processing that retains the utility/quality

of the data for learning by essentially preserving its distributional properties. We call it LCoN pre-processing since it contains Lossy Compression of Noisy data.

- 2) We present initial experimentation demonstrating the efficacy of our suggested pre-processing pipeline on the CelebA dataset not only with respect to the criteria that motivated its design, but also in providing robustness to adversarial data.

II. PRELIMINARIES

A. k -th order distribution induced by P_{X^n}

For a random n -tuple X^n , we let $Q_X^{\text{ave},(n)}$ denote the distribution of the random variable obtained by choosing one of the n components of X^n at random. More precisely, for $J \sim \text{Unif}\{1, 2, \dots, n\}$ and independent of X^n , $Q_X^{\text{ave},(n)}$ is the law of X_J . In other words, $Q_X^{\text{ave},(n)}$ is the ‘‘average’’ of the marginal laws $\{P_{X_i}\}_{i=1}^n$, and hence the superscript. We write $Q_X^{\text{ave},(n)}[P_{X^n}]$ when we want to make its dependence on the law of X^n explicit.

Similarly, for $k \leq n$, and $J \sim \text{Unif}\{1, 2, \dots, n - k + 1\}$ independent of X^n , we let $Q_{X^k}^{\text{ave},(n)}$ denote the law of the k -tuple X_J^{J+k-1} . In other words, $Q_{X^k}^{\text{ave},(n)}$ is the law obtained by averaging the marginal k -tuple laws $\left\{P_{X_i^{i+k-1}}\right\}_{i=1}^{n-k+1}$.

We write $Q_{X^k}^{\text{ave},(n)}[P_{X^n}]$ when we want to make its dependence on P_{X^n} explicit. We extend this notation in the obvious way to $Q_{X,Y}^{\text{ave},(n)} = Q_{X,Y}^{\text{ave},(n)}[P_{X^n,Y^n}]$ and $Q_{X^k,Y^k}^{\text{ave},(n)} = Q_{X^k,Y^k}^{\text{ave},(n)}[P_{X^n,Y^n}]$.

B. k -th order empirical distribution induced by x^n

For a fixed finite-alphabet n -tuple x^n , we let $Q_X^{\text{emp},(n)}[x^n]$ denote the empirical (first-order) distribution that it induces. To be precise, $Q_X^{\text{emp},(n)}[x^n]$ is a probability mass function (PMF) on the finite alphabet \mathcal{X} in which the components of x^n reside, with $Q_X^{\text{emp},(n)}[x^n](a)$ denoting the probability it assigns to $a \in \mathcal{X}$, namely the fraction of times the symbol a appears along the n -tuple x^n . To simplify the notation, we suppress the dependence on x^n , using $Q_X^{\text{emp},(n)}$ when x^n should be clear from the context.

Similarly, for $k \leq n$, $Q_{X^k}^{\text{emp},(n)}[x^n]$ denotes the empirical distribution of k -tuples along x^n . In other words, $Q_{X^k}^{\text{emp},(n)}[x^n]$ is a PMF of a k -tuple, with $Q_{X^k}^{\text{emp},(n)}[x^n](a^k)$ denoting the probability it assigns to $a^k \in \mathcal{X}^k$, the fraction of times the k -tuple a^k appears along the n -tuple x^n . Here too we suppress the dependence on x^n and write $Q_{X^k}^{\text{emp},(n)}$ when x^n should be clear from the context. We extend this notation to $Q_{X,Y}^{\text{emp},(n)} = Q_{X,Y}^{\text{emp},(n)}[x^n, y^n]$ and $Q_{X^k,Y^k}^{\text{emp},(n)} = Q_{X^k,Y^k}^{\text{emp},(n)}[x^n, y^n]$ in the obvious ways.

C. Relationship between $Q_X^{\text{ave},(n)}$ and $Q_X^{\text{emp},(n)}$

When X^n is stochastic, so is $Q_X^{\text{emp},(n)} = Q_X^{\text{emp},(n)}[X^n]$, and for any $a^k \in \mathcal{X}^k$, we have

$$\mathbb{E} \left[Q_{X^k}^{\text{emp},(n)}(a^k) \right] = Q_X^{\text{ave},(n)}(a^k). \quad (1)$$

Note further that, letting $\xrightarrow{n \rightarrow \infty}$ denote convergence in distribution, in any scenario where $Q_{X^k}^{\text{emp},(n)} \xrightarrow{n \rightarrow \infty} \mu_{X^k}$ a.s. for some PMF on k -tuples μ_{X^k} , we also have, by (1) and the bounded convergence theorem, $Q_{X^k}^{\text{ave},(n)} \xrightarrow{n \rightarrow \infty} \mu_{X^k}$. Thus, convergence of $Q_{X^k}^{\text{emp},(n)}$ is stronger than (implies) convergence of $Q_{X^k}^{\text{ave},(n)}$.

III. SAMPLES FROM THE POSTERIOR VIA NOISY LOSSY COMPRESSION

Consider the canonical setting where the components of the noise-free \mathbf{X} , noisy \mathbf{Z} , and reconstructed sources $\hat{\mathbf{X}}$ in Fig. 1 all take values in the same finite Q -ary alphabet $\mathcal{A} = \{0, 1, \dots, Q - 1\}$. The noise-free source $\mathbf{X} = (X_1, X_2, \dots)$ is stationary ergodic and corrupted by additive memoryless noise \mathbf{N} . That is, we assume the components of the noisy observation process \mathbf{Z} are given by

$$Z_i = X_i + N_i, \quad (2)$$

where the N_i s are IID $\sim N$, independent (collectively) of \mathbf{X} , and addition in (2) is in the mod- Q sense¹. We assume the distribution of the noise to be ‘‘non-singular’’ in the sense that the Toeplitz matrix whose rows are shifted versions of the row vector representing the PMF of N is invertible, a benign condition guaranteeing a one-to-one correspondence between the distributions of the noise-free and noisy sources [13]. We construct a difference distortion measure $\rho_N : \mathcal{A} \rightarrow [0, \infty]$ from the distribution of the noise according to

$$\rho_N(a) = \log \frac{1}{\text{Pr}(N = a)}. \quad (3)$$

Good lossy compression of the noisy source \mathbf{Z} under this distortion criterion at distortion level equal to the entropy of the noise ($D = H(N)$) turns out to result in reconstructions $\hat{\mathbf{X}}$ that are *samples from the posterior* of the noise-free source \mathbf{X} given the noisy source \mathbf{Z} . In particular, the finite-dimensional distributions of these reconstructions converge to those of the underlying noise-free source. We state this phenomenon rigorously in the theorem below, which follows from results in [14] (as will be detailed in the full version of this paper). ‘‘Good code’’ refers to a sequence of compressors, indexed by block-lengths, with respective rates and distortions converging to a point on the rate-distortion curve.

Theorem III.1. *Suppose \mathbf{X} is a stationary ergodic process. Let $\{\hat{X}^n\}_{n \geq 1}$ be the reconstructions associated with a good code for the source \mathbf{Z} with respect to the difference distortion function in (3), at distortion level $H(N)$. For any finite k and $n \geq k$, let $Q_{Z^k, \hat{X}^k}^{\text{ave},(n)} = Q_{Z^k, \hat{X}^k}^{\text{ave},(n)}[P_{Z^n, \hat{X}^n}]$ and $Q_{Z^k, \hat{X}^k}^{\text{emp},(n)} = Q_{Z^k, \hat{X}^k}^{\text{emp},(n)}[Z^n, \hat{X}^n]$ denote, respectively, the k -th order joint distribution induced by P_{Z^n, \hat{X}^n} and the (random)*

¹The framework and results have natural analog analogues, where the alphabet can be the real line or any Euclidean space and addition is in the usual sense. We assume here the finite alphabet setting for concreteness, for avoiding unnecessary technicalities, and because it is better connected to practice where the alphabets are ultimately finite.

k -th order joint distribution induced by the realized (Z^n, \hat{X}^n) . Then

$$Q_{Z^k, \hat{X}^k}^{\text{emp}, (n)} \xrightarrow{n \rightarrow \infty} P_{Z^k, X^k} \text{ a.s.} \quad (4)$$

and a fortiori

$$Q_{Z^k, \hat{X}^k}^{\text{ave}, (n)} \xrightarrow{n \rightarrow \infty} P_{Z^k, X^k}, \quad (5)$$

where P_{Z^k, X^k} is the joint k th-order distribution of the noisy and original noise-free source.

In particular, and most relevant for our purposes, the finite-dimensional distributions of lossy reconstructions of the noisy source converge to those of the underlying noise-free source.

IV. APPLICATION FOR LEARNING

A. Learning with Lossily Compressed Noisy Examples

Consider first the standard framework of unsupervised learning from M non-labeled examples $\{X^{n,(i)}\}_{i=1}^M$, drawn IID $\sim X^n$. The i th example comprises the data point/signal/image $X^{n,(i)}$, which is an n -tuple with \mathcal{A} -valued components. Our data pre-processing method, illustrated in Fig. 1, comprises noise injection and lossy compression to obtain and store the lossily compressed noisy (LCoN) examples, as follows:

- 1) Pick a distribution for the noise N (we discuss the choice of distribution later). Inject IID $\sim N$ noise components to each component of each of the $X^{n,(i)}$ s. Denote the noisy examples as $Z^{n,(i)}$, which are IID $\sim Z^n$, the noisy version of X^n .
- 2) Pick a good lossy compressor for the distortion function $d(z^n, \hat{x}^n) = \frac{1}{n} \sum_{i=1}^n \rho(z_i - \hat{x}_i)$ where $\rho(\cdot)$ is the distortion measure in (3) and for distortion level equal to the entropy of the noise, i.e., $D = H(N)$. Jointly compress all the noisy data. Denote the reconstructions from the lossy compression of $Z^{n,(i)}$ s as $\hat{X}^{n,(i)}$.
- 3) Use $\hat{X}^{n,(i)}$ instead of the $X^{n,(i)}$ for learning.

Although the above describes jointly compressing all the data, one may also consider a more practical version where each example is compressed separately, as we elaborate below.

B. Data Efficiency while Retaining the Right Distribution

What will be the cost of storing the compressed noisy data? Assuming the compressors employed are “good” in the sense of the previous section, it follows by invoking [14, Theorem 4] that, in the limit $M \rightarrow \infty$ of a large amount of training data, we will need a rate of

$$\frac{1}{n} H(Z^n) - H(N) \quad \frac{\text{bits}}{\text{data component}}, \quad (6)$$

namely the rate distortion function of the IID $\sim Z^n$ source at distortion level $H(N)$. Furthermore, Theorem III.1 assures us that $\{\hat{X}^{n,(i)}\}_{1 \leq i \leq M}$ will have an empirical distribution converging to the distribution of X^n when $M \rightarrow \infty$. Thus, overall, the empirical distribution of $\{\hat{X}^{n,(i)}\}_{i=1}^M$ converges in distribution to the right one, namely that of X^n . Therefore, in the limit of many training examples, performing the learning on $\{\hat{X}^{n,(i)}\}_{i=1}^M$ should be as good as performing it on the original noise-free data $\{X^{n,(i)}\}_{i=1}^M$.

We note that the foregoing discussion was valid for a fixed n and an arbitrarily distributed X^n , in the $M \rightarrow \infty$ limit. It is also meaningful to consider a fixed M in the large n limit. Indeed, when it is reasonable to think of the generic X^n governing the data as the first n components of a stationary ergodic process, even if we merely employ good compressors separately on each example, Theorem III.1 guarantees that the reconstructions will tend to be loyal to the original data in the sense of their finite-dimensional distributions, when n is large. The assumption of a stationary ergodic process governing the examples may be natural in a variety of applications, such as when the $X^{n,(i)}$ s represent audio signals or text. Also, things carry over naturally to multi-dimensionally indexed data, e.g., when the $X^{m \times n, (i)}$ s represent images sampled from the generic $X^{m \times n}$, representing the $m \times n$ grid of samples from a (spatially) stationary ergodic random field.

C. Privacy

We would also like to guarantee that the database retained for the learning does not leak too much information about any of the individual examples. To this end, we consider the (normalized) mutual information between the two, known as the *privacy leakage*, which comes with a variety of operational justifications on top of its intuitive appeal (cf. [4, 6, 7], references therein and thereto). For each i , we have

$$\begin{aligned} & \frac{1}{n} I \left(X^{n,(i)}; \left\{ \hat{X}^{n,(j)} \right\}_{j=1}^M \right) \leq \frac{1}{n} I \left(X^{n,(i)}; \left\{ Z^{n,(j)} \right\}_{j=1}^M \right) \\ & = \frac{1}{n} I \left(X^{n,(i)}; Z^{n,(i)} \right) = \frac{1}{n} I(X^n; Z^n) = \frac{1}{n} H(Z^n) - H(N), \end{aligned} \quad (7)$$

where the inequality is due to data processing and the two equalities follow by $(X^{n,(i)}, Z^{n,(i)})$ s being IID $\sim (X^n, Z^n)$.

D. Choice of the Noise Distribution

How should one choose the distribution of the noise? The higher its entropy, the smaller the respective compression rate and upper bound on the privacy leakage in (6) and (7) so, in principle, we get simultaneously better compression and more privacy. In fact, one could get both the compression rate and privacy leakage arbitrarily small with a noise distribution sufficiently close to uniform² since both (6) and (7) are upper bounded by

$$\log |\mathcal{A}| - H(N). \quad (8)$$

The choice of noise distribution, however, affects the convergence rate in large n and M limits. As a result, in practice, when both n and M are finite, there is a tension between getting good (low) compression rate plus privacy leakage and the quality (proximity to the true distribution) of the reconstructions. One might envision turning a knob sweeping through noise distributions to find a good sweet-spot. A more principled understanding of this point is left for future work.

²Uniform itself is not allowed as per the stipulation of the noise distribution being non-singular.

E. Supervised Learning

The foregoing framework and results carry over straightforwardly to the case when the noise-free data come as M labeled examples $\{(X^{n,(i)}, L_i)\}_{i=1}^M$, drawn IID $\sim (X^n, L)$, where the labels L_i take values in a finite alphabet of labels \mathcal{L} . In this case, we apply the operations and arguments discussed above separately on each subset of the data pertaining to each label value. The experimental results of Section V are in this setting.

F. When Compression is Not Matched to the Noise

The following addresses many of the natural scenarios arising in practice where the lossy compression is tailored for a distortion function and/or level not matched to the added noise characteristics.

Theorem IV.1. *Suppose the added noise is decomposable as $N = U + W$, where U and W are independent. If a good code for the source \mathbf{Z} with respect to ρ_W at distortion level $H(W)$ is utilized then $Q_{Z^k, \hat{X}^k}^{\text{emp},(n)} \xrightarrow{n \rightarrow \infty} P_{Z^k, \tilde{X}^k}$ a.s. and a fortiori $Q_{Z^k, \hat{X}^k}^{\text{ave},(n)} \xrightarrow{n \rightarrow \infty} P_{Z^k, \tilde{X}^k}$, where $\tilde{\mathbf{X}} = \mathbf{X} + \mathbf{U}$ (with \mathbf{U} IID $\sim U$ and independent of \mathbf{X}) is the partially noisy source and P_{Z^k, \tilde{X}^k} is the joint k -th-order distribution of the noisy and partially noisy source.*

Evidently, in the scenarios covered by the theorem, the lossy compression denoises \mathbf{Z} only partially. For example, when applied to the case of added Gaussian noise and compression under squared error distortion, the theorem suggests that if compression is done under distortion D smaller than the variance σ^2 of the noise then the reconstructions are effectively samples from the distribution of the noise-free data corrupted by Gaussian noise of variance $\sigma^2 - D$. The implications of this phenomenon for robustness will be explored in future work (and briefly touched on experimentally in the next section).

V. EXPERIMENTAL RESULTS

In this section, we test our suggested pipeline in the context of training a gender classifier on the CelebA dataset [3], consisting of 202,599 face images of celebrities (cf. left image in Fig. 1 for an example), using the ResNet-34 architecture [15]. We chose the CelebA dataset since privacy of face images is an emerging concern, cf., e.g., a recent work [16] studied the effect of face obfuscation in the context of the ImageNet challenge. We corrupt the original images in the CelebA dataset with (appropriately discretized) Gaussian noise. The induced distortion function in (3) with distortion level being the entropy of the noise essentially boil down to squared error with distortion level being the variance of the added Gaussian noise. The “good” lossy compressor we employ in the experiments, guided by our framework, is JPEG [17], which was (arguably) designed with squared error in mind. We tune the compression level so that the squared error distortion approximately matches the variance of the injected noise.

In Fig. 2, we compare three training schemes:

1) Our Setting - LCoN-train (orange in Fig. 2): Training over reconstructions $\hat{X}^{n,(i)}$ from Lossy Compression of Noisy

examples. We call $\hat{X}^{n,(i)}$ s as LCoN-pre-processed examples. This setting comes with guarantees on the privacy leakage and storage cost of the data, as established in the previous section. Fig. 1 exhibits $X^{n,(i)}$, $Z^{n,(i)}$ and $\hat{X}^{n,(i)}$ for a randomly chosen i at the specified noise level and corresponding distortion.

2) Baseline-1 (blue in Fig. 2): Training over the noise-free examples $X^{n,(i)}$ from the CelebA dataset. This method does not preserve privacy since the noise-free data are retained.

3) Baseline-2 (red in Fig. 2): Training over noisy examples $Z^{n,(i)}$, injected with the same noise used in LCoN-train. This time, the privacy guarantee is as good as LCoN-train’s.

After training, we test the respective three neural networks obtained (three for each noise level) on four different datasets:

1) Noise-free test images $X^{n,(i)}$ (Fig. 2(a)).

2) Noise-injected test images $Z^{n,(i)}$ – with the same noise distribution used for the training data (Fig. 2(b)).

3) LCoN-pre-processed test images $\hat{X}^{n,(i)}$ – with the same noise and distortion used for the training data (Fig. 2(c)).

4) Adversarial test images – generated via the Fast Gradient Sign Method (FGSM) [12] (Fig. 2(d)).

In Fig. 2(a-c), PSNR refers to the PSNR of the noisy images (as dictated by the noise variance) after noise injection, prior to lossy compression. For a fair comparison, we calibrate the number of examples used by each scheme so that the overall storage cost (in bits) is approximately the same. In other words, in Fig. 2(a-c), the points on the same vertical line (same PSNR, same privacy) are trained with examples requiring the same storage cost by adjusting the number of training examples used. The compression rate for each point is provided in the title of Fig. 2. In Fig. 2(d), we vary the parameter ϵ in FGSM. Recall that FGSM corrupts the data as $x_{\text{adv}} = x + \epsilon \cdot \text{sign}(\nabla_x J)$, where J is the loss function of the downstream task, i.e., the higher ϵ the more corrupted the adversarial data. In Fig. 2(d), in addition to testing directly on the adversarial data, we test LCoN-train and Baseline-1 on LCoN-pre-processed adversarial data as well. We denote the pre-processed adversarial data as LCoN-adv (empty markers).

We observe that LCoN-train consistently outperforms Baseline-2 in all settings and noise levels. The gap is most significant when the models are tested on the noise-free images (Fig. 2(a)). This behavior is expected in light of the theory exposed in the previous sections: LCoN examples $\hat{X}^{n,(i)}$ are close in distribution to the noise-free examples $X^{n,(i)}$ so a model trained on LCoN examples should be expected to outperform one trained on the noisy ones $Z^{n,(i)}$. Perhaps less expected is that LCoN-train outperforms Baseline-2 even on the noisy data on which the latter was trained. The comparison to Baseline-1 is also extremely favorable (on top of the fact that Baseline-1 preserves no privacy) essentially across the deck. Even on the noise-free test data, our method yields essentially the same accuracy as Baseline-1 at sufficiently high PSNR. Remarkably, our setting reaches 96.8% accuracy for PSNR higher than 20 dB, which is even higher than the 96.6% accuracy of the model trained with full noise-free CelebA dataset (not a subset to comply with the storage constraint, as in Baseline-1). Evidently, even when storage is free and

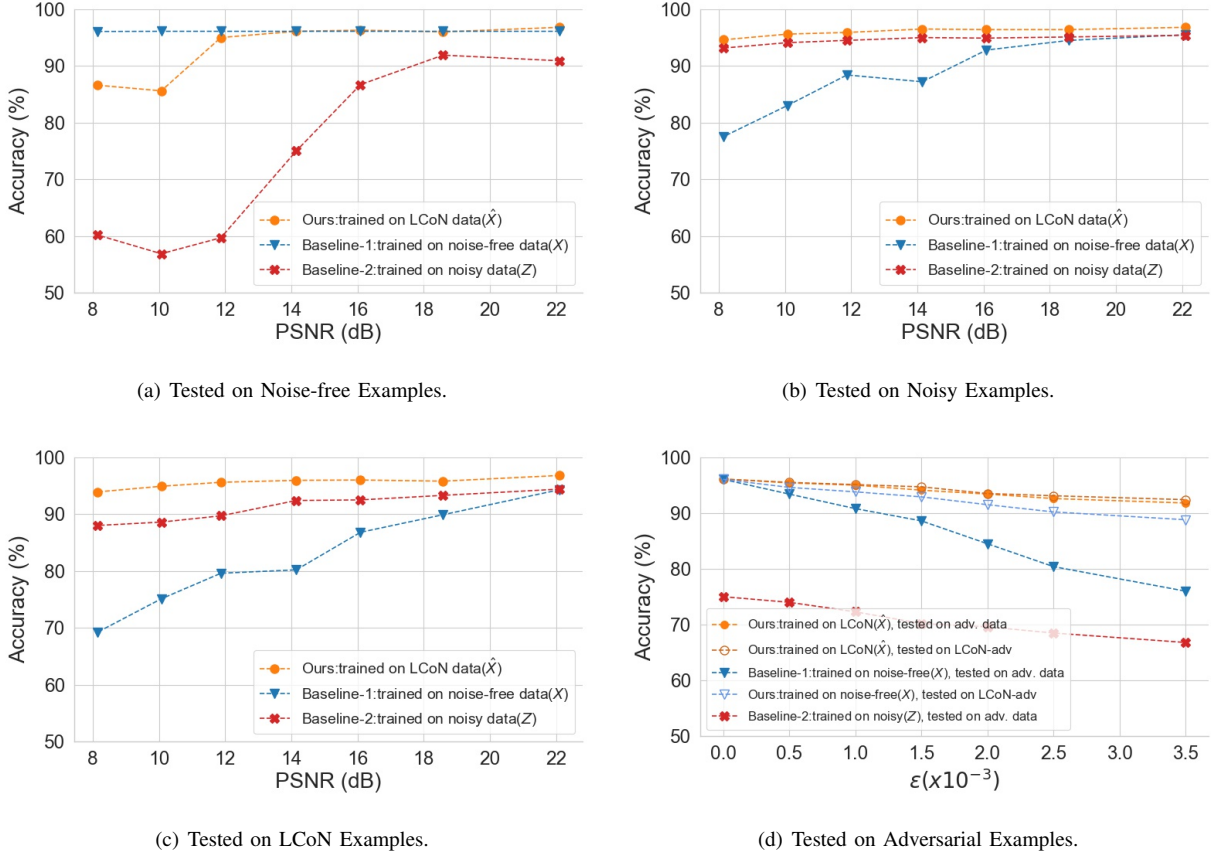


Fig. 2. Comparison of models trained with LCoN examples, noise-free examples, and noisy examples on (a) noise-free test examples, (b) noisy test examples, (c) LCoN test examples, (d) adversarial test examples. Adversarial images are generated via the Fast Gradient Sign Method (FGSM) [12]. The compression rates of LCoN for PSNR [8.1, 10.1, 11.9, 14.2, 16.1, 18.6, 22.1] in (a-c) are [0.131, 0.136, 0.160, 0.170, 0.173, 0.179, 0.200], respectively.

privacy is not an issue, LCoN-train is an accuracy booster. Finally, Fig. 2(d) shows that LCoN-train is a significant performance booster in the face of adversarially corrupted data as well. The gap between LCoN-train and the better of the other two benchmarks becomes as large as 16.4% in accuracy. Furthermore, even if the model is trained on the noise-free data, LCoN pre-processing of the adversarial testing data can result in as much as 13% of an accuracy boost. Overall, it seems, LCoN pre-processing is advisable both at training and testing (and at just one of them if the other is fixed).

Lastly, Fig. 3 shows that the best accuracy (across all test data sets) is obtained when the distortion level (mse) is closest to the entropy of the noise. For all the points in Fig. 3, a $N(0, 1600)$ Gaussian noise is added to the training data. The black vertical line corresponds to $\text{mse} = 1600$ where the distortion level is matched to the entropy of the noise. As expected from Theorem IV.1, when the distortion level decreases, the lossily reconstructed examples $\tilde{X}^{n,(i)}$ the model is trained on become more noisy. This results in a model trained on examples with distribution further away from the distribution of the $X^{n,(i)}$ s, explaining the significant accuracy drop, especially on the noise-free test data, when $D < H(N)$. A similar effect occurs when $D > H(N)$.

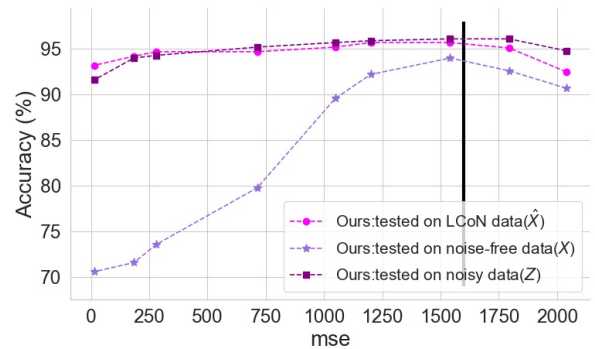


Fig. 3. LCoN-train with training data added Gaussian noise $N(0, 1600)$ and compressed with varying distortion levels (mse). Vertical line corresponds to $\text{mse} = 1600$, where the distortion level and the entropy of the noise are matched.

VI. CONCLUSION AND FUTURE WORK

Guided by and combining existing theory on lossy noisy data compression and on information-theoretic privacy, we proposed a data pre-processing procedure for both training and testing data which appears to simultaneously boost data efficiency, privacy, accuracy and robustness. Our theoretical

framework has accounted for much of the empirical observations as they pertain to the efficiency (compression), privacy (leakage) and accuracy (due to preservation of the right distribution). The robustness is a welcome additional feature we have observed empirically, and perhaps to be intuitively expected given empirical work showing that noise injection [18] and image compression [19, 20, 21], when applied to adversarial data (each separately), improves robustness. Future work will be dedicated to quantifying this effect via (an extension of) our theoretical framework. From a high-level perspective, LCoN and dithered quantization [22] have some resemblance in injecting noise prior to compression. However, we employ noise injection, independent of the lossy compression, to preserve privacy while the added noise in dithered quantization is an essential component of the quantization step. We also note that our framework and theoretical insights transfer directly to the case where the data is noise-corrupted to begin with (rather than the noise being deliberately injected). In such a case, the compression would be tuned to the real noise characteristics. Practically, we plan to further the experiments to other noise distributions and image compressors such as PNG [23], JPEG XR [24], WebP [25] and LZZip [26], which would be equally natural to experiment with, so long as they are appropriately matched (Gaussian noise for compressors designed with squared error in mind, Laplacian noise for compressors optimized for absolute error, Uniform distribution on a sub-interval of length equal to the allowed maximum distortion for compressors designed under a maximal distortion criterion such as LZZip [26], etc.). Better compressors will likely boost the performance under the other criteria as well.

VII. ACKNOWLEDGEMENT

This work was supported in part by a Sony Stanford Graduate Fellowship.

REFERENCES

- [1] M. I. Jordan and T. M. Mitchell, "Machine learning: Trends, perspectives, and prospects," *Science*, vol. 349, no. 6245, pp. 255–260, 2015.
- [2] A. Krizhevsky, I. Sutskever, and G. E. Hinton, "Imagenet classification with deep convolutional neural networks," *Advances in neural information processing systems*, vol. 25, pp. 1097–1105, 2012.
- [3] Z. Liu, P. Luo, X. Wang, and X. Tang, "Deep learning face attributes in the wild," in *Proceedings of International Conference on Computer Vision (ICCV)*, December 2015.
- [4] A. Makhdoumi, S. Salamatian, N. Fawaz, and M. Médard, "From the information bottleneck to the privacy funnel," in *2014 IEEE Information Theory Workshop (ITW 2014)*. IEEE, 2014, pp. 501–505.
- [5] L. Sankar, S. R. Rajagopalan, and H. V. Poor, "Utility-privacy tradeoffs in databases: An information-theoretic approach," *IEEE Transactions on Information Forensics and Security*, vol. 8, no. 6, pp. 838–852, 2013.

- [6] F. du Pin Calmon and N. Fawaz, "Privacy against statistical inference," in *2012 50th annual Allerton conference on communication, control, and computing (Allerton)*. IEEE, 2012, pp. 1401–1408.
- [7] A. Makhdoumi and N. Fawaz, "Privacy-utility trade-off under statistical uncertainty," in *2013 51st Annual Allerton Conference on Communication, Control, and Computing (Allerton)*. IEEE, 2013, pp. 1627–1634.
- [8] K. Chatzikokolakis, T. Chothia, and A. Guha, "Statistical measurement of information leakage," in *International Conference on Tools and Algorithms for the Construction and Analysis of Systems*. Springer, 2010, pp. 390–404.
- [9] D. Rebollo-Monedero, J. Forne, and J. Domingo-Ferrer, "From t-closeness-like privacy to postrandomization via information theory," *IEEE Transactions on Knowledge and Data Engineering*, vol. 22, no. 11, pp. 1623–1636, 2009.
- [10] C. Huang, P. Kairouz, X. Chen, L. Sankar, and R. Rajagopal, "Generative adversarial privacy," *arXiv preprint arXiv:1807.05306*, 2018.
- [11] R. McPherson, R. Shokri, and V. Shmatikov, "Defeating image obfuscation with deep learning," *arXiv preprint arXiv:1609.00408*, 2016.
- [12] I. Goodfellow, J. Shlens, and C. Szegedy, "Explaining and harnessing adversarial examples," in *International Conference on Learning Representations*, 2015. [Online]. Available: <http://arxiv.org/abs/1412.6572>
- [13] T. Weissman, E. Ordentlich, G. Seroussi, S. Verdú, and M. J. Weinberger, "Universal discrete denoising: Known channel," *IEEE Transactions on Information Theory*, vol. 51, no. 1, pp. 5–28, 2005.
- [14] T. Weissman and E. Ordentlich, "The empirical distribution of rate-constrained source codes," *IEEE transactions on information theory*, vol. 51, no. 11, pp. 3718–3733, 2005.
- [15] K. He, X. Zhang, S. Ren, and J. Sun, "Deep residual learning for image recognition," in *Proceedings of the IEEE conference on computer vision and pattern recognition*, 2016, pp. 770–778.
- [16] K. Yang, J. Yau, L. Fei-Fei, J. Deng, and O. Russakovsky, "A study of face obfuscation in imagenet," *arXiv preprint arXiv:2103.06191*, 2021.
- [17] W. B. Pennebaker and J. L. Mitchell, *JPEG: Still image data compression standard*. Springer Science & Business Media, 1992.
- [18] A. Kurakin, I. Goodfellow, and S. Bengio, "Adversarial examples in the physical world," *ICLR Workshop*, 2017. [Online]. Available: <https://arxiv.org/abs/1607.02533>
- [19] G. K. Dziugaite, Z. Ghahramani, and D. M. Roy, "A study of the effect of jpg compression on adversarial images," *arXiv preprint arXiv:1608.00853*, 2016.
- [20] N. Das, M. Shanbhogue, S.-T. Chen, F. Hohman, L. Chen, M. E. Kounavis, and D. H. Chau, "Keeping the bad guys out: Protecting and vaccinating deep learning with jpeg compression," *arXiv preprint arXiv:1705.02900*, 2017.

- [21] Z. Liu, Q. Liu, T. Liu, N. Xu, X. Lin, Y. Wang, and W. Wen, "Feature distillation: Dnn-oriented jpeg compression against adversarial examples," in *2019 IEEE/CVF Conference on Computer Vision and Pattern Recognition (CVPR)*. IEEE, 2019, pp. 860–868.
- [22] R. M. Gray and T. G. Stockham, "Dithered quantizers," *IEEE Transactions on Information Theory*, vol. 39, no. 3, pp. 805–812, 1993.
- [23] G. Roelofs, *PNG: the definitive guide*. O'Reilly Media, 1999.
- [24] F. Dufaux, G. J. Sullivan, and T. Ebrahimi, "The jpeg xr image coding standard [standards in a nutshell]," *IEEE Signal Processing Magazine*, vol. 26, no. 6, pp. 195–204, 2009.
- [25] G. Ginesu, M. Pintus, and D. D. Giusto, "Objective assessment of the webp image coding algorithm," *Signal Processing: Image Communication*, vol. 27, no. 8, pp. 867–874, 2012.
- [26] S. Chandak, K. Tatwawadi, C. Wen, L. Wang, J. Aparicio, and T. Weissman, "Lfzip: Lossy compression of multivariate floating-point time series data via improved prediction," in *Proceedings of the Data Compression Conference (DCC)*, 2020, pp. 342–351.